Journal of ELECTRONIC MATERIALS, Vol. 38, No. 6, 2009
DOI: 10.1007/s11664-009-0741-3

Regular Issue Paper

Aqueous-Develop, Photosensitive Polynorbornene Dielectric: Properties and Characterization

VENMATHY RAJARATHINAM,[1,3] C. HUNTER LIGHTSEY,[1] TYLER OSBORN,[1] BRIAN KNAPP,[2] EDMUND ELCE,[2] SUE ANN BIDSTRUP ALLEN,[1] and PAUL A. KOHL[1]

1.—School of Chemical and Biomolecular Engineering, Georgia Institute of Technology, 311 Ferst Drive, Atlanta, GA 30332-0100, USA. 2.—Promerus LLC, 9921 Brecksville Road, Brecksville, OH 44141, USA. 3.—e-mail: gth799x@mail.gatech.edu

The properties of a new aqueous-base-develop, negative-tone photosensitive polynorbornene have been characterized. High-aspect-ratio features of 7:1 (height:width) were produced in 70-μm-thick films in a single coat with straight side-wall profiles and high fidelity. The polymer films studied had contrast of 12.2 and low absorption coefficient. To evaluate the polymer's suitability to microelectronics applications, epoxy crosslinking reactions were studied as a function of processing condition through Fourier-transform infrared spectroscopy, nanoindentation, and dielectric measurements. The fully crosslinked films had an elastic modulus of 2.9 GPa and hardness of 0.18 GPa.

Key words: Crosslinking, dielectric properties, polynorbornenes, nanoindentation

INTRODUCTION

Polymers are widely used in the microelectronics industry as thin-film, dielectric layers with copper in substrates and packages, and as passivation layers on semiconductor devices. Epoxy-based polymers are particularly useful in electronic packaging because they have excellent adhesion and react at modest temperatures. Extensive research has been conducted to establish structure–property relationships with epoxy-based polymers such as Avatrel® 2000P (Promerus LLC) and SU-8 (MicroChem).[1–5]

Avatrel 2000P is a copolymer of alkyl norbornene and epoxide-functionalized norbornene monomers, as shown in Fig. 1. The properties of the polymer film can be controlled by varying the alkyl-to-epoxy ratio. The alkyl side-groups have been shown to lower the elastic modulus and increase the elongation to break, and the epoxide side-groups provide crosslinkable sites, increase adhesion characteristics, and increase elastic modulus.[4]

(Received November 25, 2008; accepted February 18, 2009; published online March 19, 2009)

SU-8, shown in Fig. 2, is an epoxy-based resin initially developed by IBM and designed for microelectromechanical systems (MEMS).[6,7] The resin has a low molecular weight and can be dissolved in a variety of organic solvents.[8] It has a high degree of functionality with good mechanical properties and high chemical and thermal resistance.[5] The final properties of SU-8 are sensitive to processing conditions and the reported properties have some variability.[9–13]

A challenging application space exists for photosensitive, thick-film, high-aspect-ratio polymers in microelectronics applications and MEMS. In this work, characterization has been performed on Avatrel 8000P (Promerus LLC) a new high-aspect-ratio, aqueous-base-develop, photosensitive polymer. Avatrel 8000P, shown in Fig. 3, consists of a norbornene backbone with fluorinated alcohol groups which provide solubility in an aqueous base and carboxylic acid groups which provide crosslinking sites with epoxy units. The polymer formulation is a mixture containing a multifunctional epoxy crosslinker, a photocatalyst, and an adhesion promoter.

The contrast and optical properties were studied and compared with Avatrel 2000P and SU-8 to

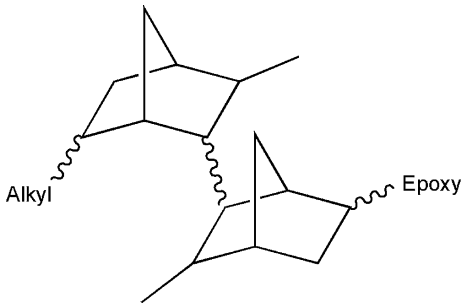

Fig. 1. The chemical structure of Avatrel 2000P.

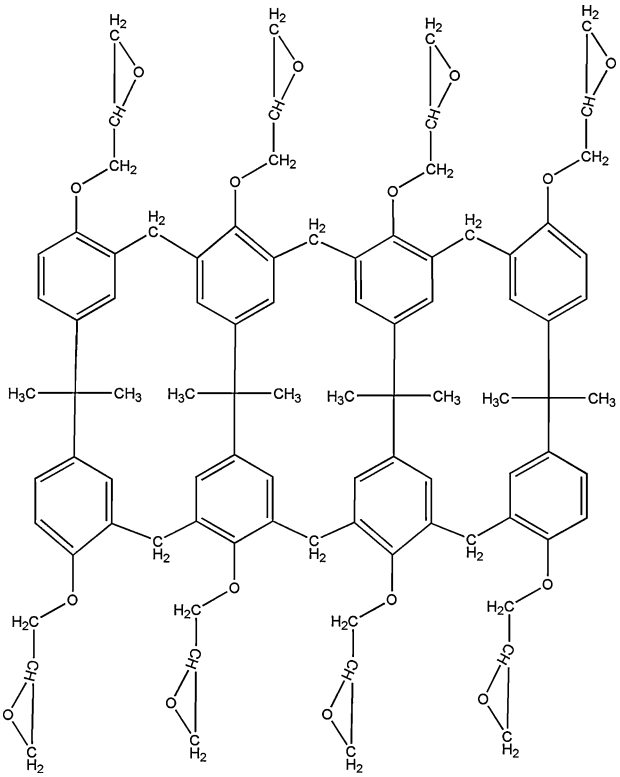

Fig. 2. The chemical structure of SU-8.

understand better the high aspect ratio of the patterned films. The impact of curing condition and exposure dose on the mechanical, thermal, and electrical properties of Avatrel 8000P has been evaluated. The relationship between processing conditions and material properties were examined to optimize the processing conditions in order to obtain a high-quality Avatrel 8000P film. Additionally, the impact of the different polymer structures of Avatrel 2000P, SU-8, and Avatrel 8000P on material properties and performance is discussed.

EXPERIMENTAL

Avatrel 2000P was processed according to the procedures of Bai et al.,[3,4] and SU-8 was processed according to the procedures listed on the MicroChem website.[14] Avatrel 8000P samples were

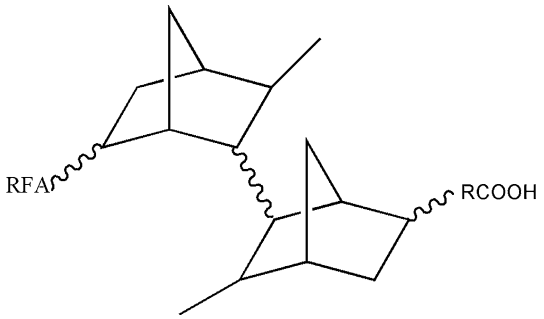

Fig. 3. The chemical structure of Avatrel 8000P; RFA = hydroxyl(polyfluoro)alkyl.

spin-coated onto ⟨100⟩ silicon wafers and then soft-baked on a hotplate at 100°C for 5 min to remove the solvent from the polymer film. A variable-density optical mask (Opto-line International Inc.) was used to study the effect of dose on polymer properties. A 1-kW Hg-Xe lamp with a 365-nm filter was used for ultraviolet (UV) exposure, and the post-exposure bake was performed on a hotplate at 100°C for 5 min. The Avatrel 8000P films were developed in MF-319 (Shipley) which contained tetramethylammonium hydroxide (TMAH) and a surfactant. Curing was performed in a nitrogen-purged furnace, and the samples were ramped to their cure temperature at 5°C/min and held at temperature for 1 h. The furnace was allowed to cool slowly by natural convection to room temperature.

A Zeiss Ultra 60 was used to obtain scanning electron microscope (SEM) images of the processed films. Film thicknesses were measured with a Veeco Dektak profilometer, and UV absorption was measured on quartz wafers with a Hewlett Packard 8543 UV–vis spectrophotometer. The residual film stress in polymer films was measured at room temperature using the Flexus Tencor F2320. Weight loss due to temperature exposure was measured using a TA Instruments Q50 thermogravimetric analyzer (TGA). The temperature inside the sample chamber was increased at a rate of 5°C/min or 0.5°C/min from 27°C to 500°C under N_2 atmosphere.

Quasistatic nanoindentation was conducted on polymer samples using a Hysitron Triboindenter with a Berkovich tip. The peak load was varied between 250 μN and 7500 μN over a 5 × 5 array of points per sample. A maximum drift rate of 0.1 nm/s was set for the experiment and was automatically determined over a 40 s period. The tip was loaded to maximum load in 10 s, held for 10 s, and unloaded in 2 s. The load–depth curves were analyzed for the 25 points using the Oliver–Pharr model.[15] The reduced modulus (E_r) was extracted from 20% to 95% of the unloading curve and the hardness (H) was obtained by using Eqs. 4–6. The samples were indented in the central regions of the polymer samples to eliminate edge effects. Additionally, to minimize the impact of thermal drift, the first five

points were discarded, and subsequently only indents above 500 nm were included in the average modulus and hardness presented.

The ring-opening reaction of epoxide groups with the polymer was measured by Fourier-transform infrared (FT-IR) spectroscopy using a Magna 560 spectrometer (Nicolet Instruments). FT-IR scans of samples were collected in transmission mode on KBr crystals, and for each measurement 512 scans at a resolution of 2.00 cm^{-1} were averaged. Specifically, the change in the peak at 844 cm^{-1}, associated with the C–O–C stretching, was used to monitor conversion. Dielectric measurements were performed by fabricating parallel-plate capacitors. The bottom plate of the capacitors was a full-surface metal film of sputtered Ti/Au/Ti (300 Å/4000 Å/300 Å) using the Unifilm sputtering system. The top electrode consisting of Ti/Au/Ti (300 Å/4000 Å/300 Å) was patterned by photolithography and wet etching. Capacitance and conductance were measured at 10 kHz using a Hewlett Packard 4236 LCR meter on a Karl Suss probe station. No correction was needed for fringing fields around the perimeter of the capacitors due to the high capacitor area-to-thickness ratio (>1000).[16]

CHARACTERIZATION

The contrast (γ) of the photosensitive polymer was obtained by measuring film thickness after developing as a function of exposure dose. Equation 1 describes the relationship between exposure dose and contrast:

$$\gamma = \frac{1}{\log_{10}(D_{100}/D_0)}, \tag{1}$$

where D_{100} is the exposure dose at which none of the photodefined material is removed upon exposure to developer, and D_0 is the exposure dose at which all of the photodefined material is removed. Mathematically γ represents the slope of the linear region of a plot of normalized film thickness versus the log of exposure dose.

Stoney's equation is used to relate the residual stress of a film to the change in the radius of curvature of the supporting substrate:

$$\sigma = \left(\frac{E}{1-\upsilon}\right)\frac{h^2}{6Rt}, \tag{2}$$

where σ is the residual stress, $E/1-\upsilon$ is the biaxial elastic modulus of the substrate (1.805×10^{11} Pa for $\langle 100\rangle$-oriented silicon), t is the thickness of the film, and h is the substrate thickness. R is the reduced change in radius, given by

$$\frac{1}{R} = \frac{1}{R_2} - \frac{1}{R_1}, \tag{3}$$

where R_1 is the radius of curvature of the uncoated substrate and R_2 is the radius of curvature of the substrate after film coating and processing. According to Klein, Stoney's equation correctly represents the average biaxial stress acting within a film deposited on a substrate for film thicknesses less than 10% of the substrate thickness.[17]

Nanoindentation is a depth sensing technique used to characterize mechanical properties such as reduced modulus and hardness. It has been used to characterize materials such as ceramics,[18] biological specimens,[19] and metallic alloys.[20,21] However, the nanoindentation of polymers is particularly challenging due to their significant compliance and low hardness,[22] viscoelastic or viscoplastic response,[23] and resulting strain-rate dependence of deformation.[24]

The hardness is defined as applied load per unit area of indentation. For a maximum load of P_{max} and a projected contact area of $A(h_c)$ as a function of contact depth h_c, the indentation hardness is defined as

$$H = \frac{P_{max}}{A(h_c)}. \tag{4}$$

The gradient of the initial portion of the unloading stiffness curve provides the elastic parameters of the material given that the creep effects are dissipated through a hold.[15] The gradient or unloading stiffness (S) is given by:

$$S = \frac{dP}{dh}. \tag{5}$$

A key challenge in interpreting indentation results is the determination of $A(h_c)$. Oliver and Pharr,[15] estimate h_c for a geometrical constant (ε) from

$$h_c = h_{max} - \varepsilon\frac{P_{max}}{S}. \tag{6}$$

The value of E_r is expressed by

$$\frac{1}{E_r} = \frac{(1-\upsilon_m^2)}{E_m} + \frac{(1-\upsilon_i^2)}{E_i}, \tag{7}$$

where E and υ are the elastic modulus and the Poisson's ratio, respectively, and the subscripts "m" and "i" refer to the material and the indenter, respectively. The relationship between S and E_r is given by

$$S = 2aE_r = \frac{2\beta E_r\sqrt{A}}{\sqrt{\pi}}, \tag{8}$$

where β is a constant and the ideal area function of a Berkovich tip is represented by $A = 24.5h_c^2$. For an indenter with a tip imperfection, the area is described by

$$A(h_c) = 24.5h_c^2 + \sum_{i=0}^{7} a_i h_c^{1/2^i}. \tag{9}$$

The extended coefficients (a_i) for the area function are typically found by performing indents over a range of depths in a material of known modulus.

Fused silica (quartz) is commonly used as a standard because its elastic modulus does not vary significantly with depth and does not have a surface layer such as a surface oxide in metals.[25] However, researchers have shown that it is necessary to calibrate with a standard having a modulus similar to the sample so that the area function obtained from the standard is valid over the indentation depths of the sample.[26] A polycarbonate calibration standard (Hysitron Inc.) with a modulus of 3.1 GPa was used to calculate the area function for the measurements presented in this work.

RESULTS AND DISCUSSION

Photodefinable polymers with high contrast and high sensitivity are valuable because of their ability to form thick, high-aspect-ratio polymer structures. The polymer structures must also have high mechanical strength and excellent optical properties to be suitable for MEMS and microelectronics applications. The spin speed versus thickness curve in Fig. 4 illustrates that thick Avatrel 8000P films above 100 μm can be obtained in a single coat. Avatrel 8000P samples were baked for 5 min before and after exposure at 100°C, whereas SU-8 requires longer processing times and temperature ramping steps for comparable film thicknesses. Avatrel 8000P was spun at 750 rpm and photopatterned with an exposure dose of 500 mJ/cm^2; the resulting 70-μm features are shown in Fig. 5. The lines in the SEM image have a high aspect ratios of 7:1 (height:width) with smooth, straight side-wall profiles. Avatrel 8000P was also evaluated for its ability to make complex shapes; Fig. 6 shows a hollow-core cylindrical structure fabricated with the same processing conditions. The aspect ratio in Fig. 6 is 5:1 (height:width) where the inside diameter of the core corresponds to the width dimension. The aspect ratio of the hollow structure is lower than the aspect ratio of the solid structure, because delamination occurred in cylinders with aspect ratios above 5:1. In high-aspect-ratio hollow structures, the transport of the developer in the core is slow compared with the transport of developer around the perimeter of the feature. As a result, hollow structures required longer develop times than solid features of comparable aspect ratios, which caused delamination of features with aspect ratios above 5:1. The structures in Fig. 5 have a slight nonvertical slope, but the hollow pillar in Fig. 6 suggests that the taper is minimal. Sidewall slope may occur in thick, high-aspect-ratio structures due to UV absorbance in the film. Negative-sloped sidewalls can be mitigated by using a filter to remove shorter wavelengths that are absorbed in the upper portion of the polymer and by optimizing the exposure dose and baking conditions to obtain a uniform crosslink density throughout the film.[27]

The contrast value of thick Avatrel 8000P films was measured to understand better the limitations of the material to pattern high-aspect-ratio features. Contrast is an important parameter for photoresists and is usually measured in thin films. Although contrast normally decreases with

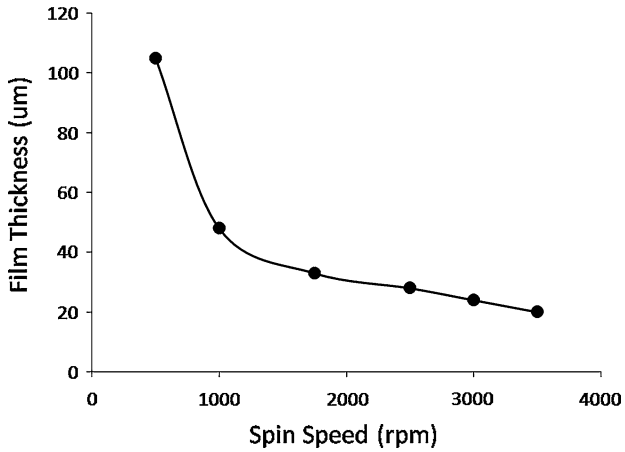

Fig. 4. Avatrel 8000P spin speed versus thickness curve.

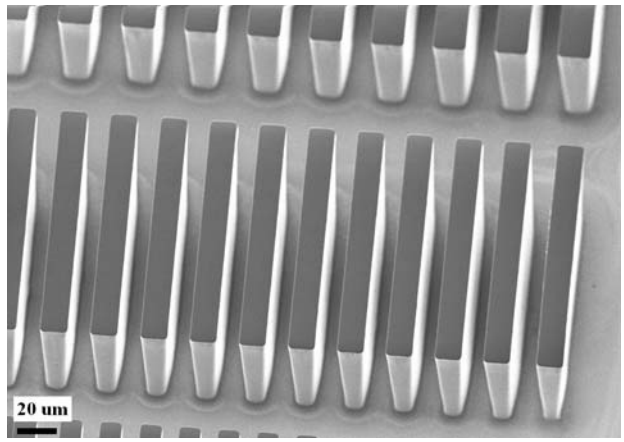

Fig. 5. SEM image of 7:1 (height:width) Avatrel 8000P lines photopatterned with an exposure dose of 500 mJ/cm^2.

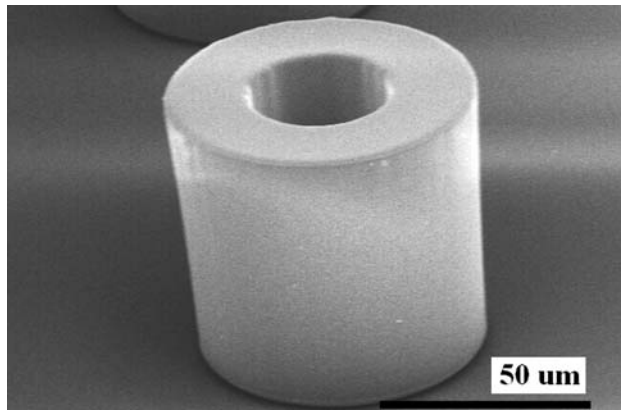

Fig. 6. SEM image of a 5:1 (height:width) Avatrel 8000P hollow-core cylinder photopatterned with an exposure dose of 500 mJ/cm^2.

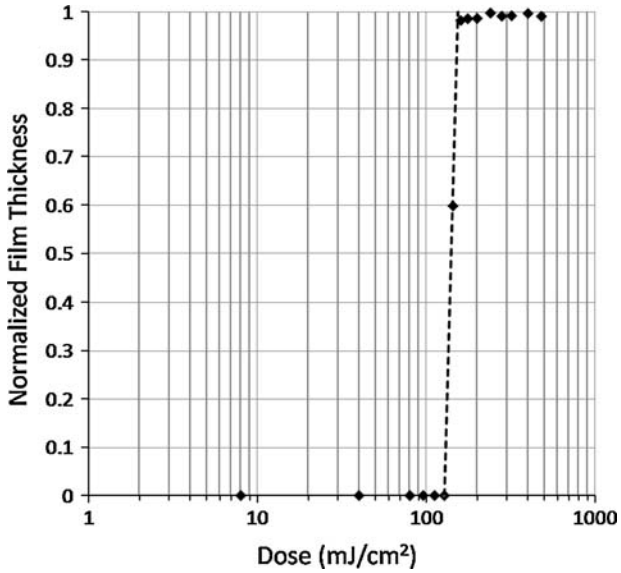

Fig. 7. Contrast curve for thick Avatrel 8000P films obtained using front-side exposure (γ = 12.2).

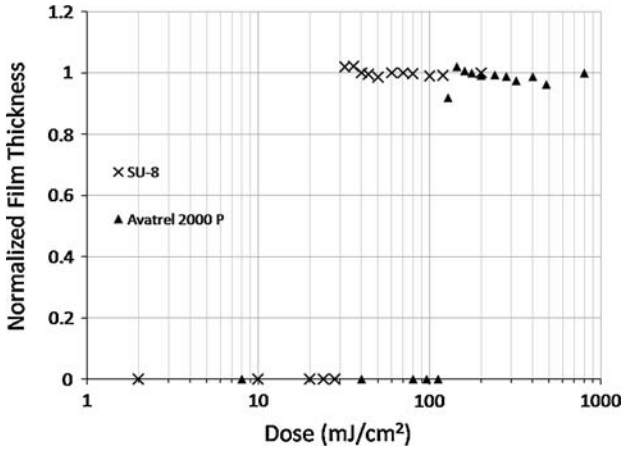

Fig. 8. Contrast curve for thick Avatrel 2000P and SU-8 films obtained using front-side exposure.

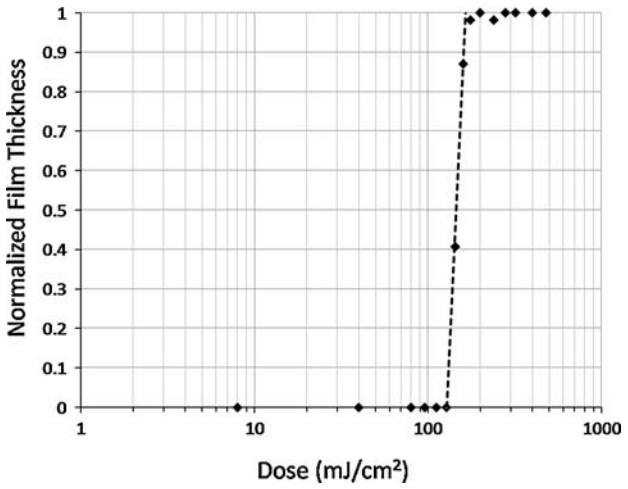

Fig. 9. Contrast curve for thick Avatrel 8000P films obtained using back-side exposure (γ = 9.04).

increasing film thickness, the contrast value for Avatrel 8000P was high (γ = 12.2). Figure 7 shows the contrast curve for a thick film of Avatrel 8000P using front-side exposure, and a least-squares method was used to fit the slope of the line from D_0 to D_{100} (Eq. 1). Measuring contrast using front-side exposure is appropriate for processing applications, but the accuracy of the contrast is limited by the number of obtainable data points between D_0 and D_{100}. Contrast measurements are traditionally conducted in thin films in which dose can be considered relatively constant through the film thickness. However, in thick films, the exposure dose at the top of a feature is higher than the dose at the bottom of a feature due to absorption of UV light within the film. Also, the crosslink density can affect the swelling and dissolution of the film. Obtaining data points between D_0 and D_{100} is particularly difficult for negative-tone, thick-film polymers. For comparison, contrast measurements were conducted using front-side exposure for SU-8 and Avatrel 2000P as shown in Fig. 8. In these figures, the films irradiated with doses near D_{100} suffer from delamination due to poor substrate adhesion and high film stress. The contrast values are not reported due to the difficulty in determining the exact value of D_{100} due to delamination. The sensitivity of SU-8 and Avatrel 2000P are 40 mJ/cm^2 and 176 mJ/cm^2, respectively.

A series of back-side exposures were performed to evaluate the impact of adhesion on the contrast values. Irradiating the polymer through a UV-transparent substrate results in the highest exposure dose and highest level of crosslinking at the polymer–substrate interface. Since the swelling and/or dissolution rate near the bottom of a feature was less than the top surface with back-side exposure, more data points could be collected between D_0 and D_{100}. Figure 9 shows the contrast curve obtained for Avatrel 8000P through back-side exposure and, after curve-fitting, the contrast was found to be 9.04. The lower contrast value obtained from backside exposure is attributed to the shift in the D_0 and D_{100} doses. The shift of D_0 and D_{100} occurs because the level of crosslinking at the top and bottom of the film differ from the case of front-side exposure, resulting in different dissolution rates for the two exposure methods.

As previously mentioned, the absorption coefficient of a photodefinable material impacts its resolution and ability to make high-aspect-ratio features in thick films. Eyre et al. have shown that, if the optical absorption of a photoresist is too high, UV light will not penetrate a thick resist layer and therefore clean, sharp images cannot be generated.[28] The absorption coefficient of fully formulated Avatrel 8000P (i.e., with epoxy-functionalized crosslinker, and photopackage) was measured after

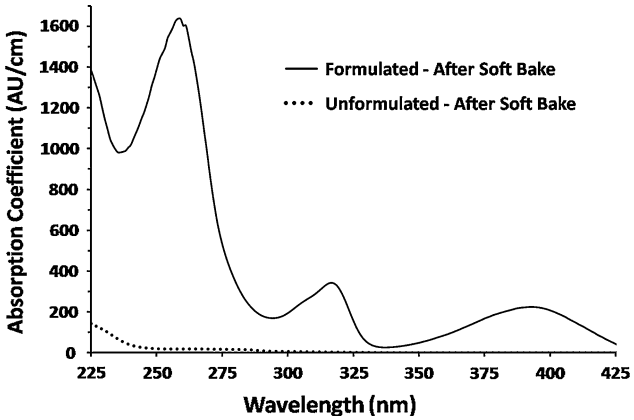

Fig. 10. Changes in the absorption coefficient of fully formulated Avatrel 8000P and pure norbornene Avatrel 8000P from 225 nm to 425 nm.

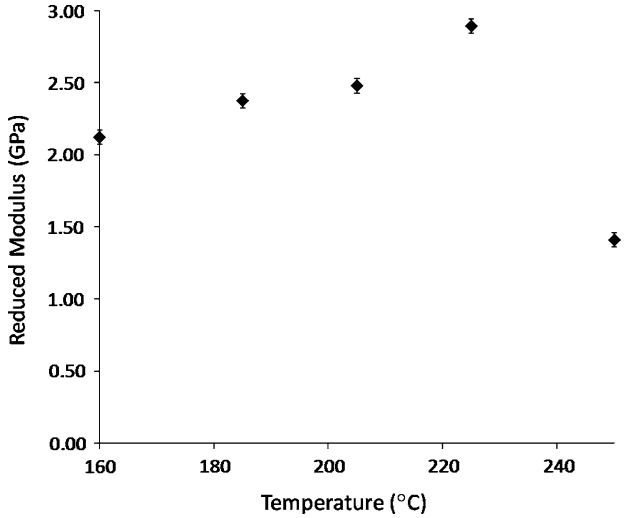

Fig. 11. The reduced modulus of Avatrel 8000P as a function of cure temperatures from 160°C to 250°C.

soft-bake, exposure, and post-exposure bake. As shown in Fig. 10, the absorption coefficient at 365 nm is 110 cm^{-1} after soft bake and 94 cm^{-1} after post-exposure bake. The decrease in absorption coefficient is due to decomposition of the photocatalyst after exposure, which lowers the concentration of the absorbing species. To evaluate only the contribution of the norbornene copolymer, the absorption coefficient of the norbornene copolymer was measured in propylene glycol monomethyl ether acetate (PGMEA). At 365 nm, the absorption coefficient is 0.25 cm^{-1}, indicating that the norbornene molecule absorbs a small amount of photons compared with the photopackage. Thus, the high aspect ratios of the patterned Avatrel 8000P films are a result of the high contrast values and low absorption coefficient.

Osborn et al. have conducted a brief mechanical comparison of Avatrel 2000P, Avatrel 8000P, and SU-8 through nanoindentation. Avatrel 2000P was the softest material with a modulus of 1.0 GPa whereas SU-8 and Avatrel 8000P had comparable modulus values of 3.3 GPa and 3.1 GPa, respectively.[29] To evaluate the suitability of Avatrel 8000P as a permanent dielectric in MEMS and microelectronics applications, the impact of processing on the mechanical properties of Avatrel 8000P were analyzed using nanoindentation. Avatrel 8000P samples were indented after soft bake and after an exposure dose of 500 mJ/cm^2, and the modulus of the soft-baked and exposed films were 1.1 GPa and 1.3 GPa, respectively. A sample indented after postexposure bake had variation in modulus values over the top few microns of the film's surface. To assess the film properties of Avatrel 8000P, a sample was indented from the backside of the film and a modulus of 1.8 GPa was obtained.

To evaluate the impact of cure temperature on Avatrel 8000P's reduced modulus, cure temperatures from 160°C to 250°C were investigated. As shown in Fig. 11, modulus values increased nearly 40% from 160°C to 225°C; this increase is attributed to a higher crosslink density as the cure temperature increased. Chiniwalla et al. found that the final extent of epoxy ring opening is greater at higher temperatures due to an increased diffusion coefficient of the photocatalyst and reactive groups, leading to improved network interconnectivity.[1] At 250°C, Avatrel 8000P's decomposition reactions occur at a faster rate than the crosslinking reactions, resulting in lower modulus.

An Avatrel 8000P sample originally cured at 225°C had a modulus of 2.9 GPa and, after being subjected to a second cure for 2 h at 250°C, it had a modulus of 2.5 GPa. The modest rate of decrease in modulus with time at the elevated temperature suggests that the crosslinking groups are difficult to break once formed, resulting in high thermal stability of the crosslinked film. Avatrel 2000P and Avatrel 8000P samples were also indented after a 160°C cure and after an extended cure of the same samples for an additional 10 h at the same temperatures. After the 160°C cure for 1 h, Avatrel 8000P and Avatrel 2000P had a reduced modulus of 2.1 GPa and 0.6 GPa, respectively. After the extended cure, the modulus of Avatrel 8000P and Avatrel 2000P both drop by 50%. The loss in modulus is attributed to the loss of linkages through thermal decomposition. Chiniwalla et al. have shown that decomposition reactions associated with an epoxide side-group can occur at temperatures greater than 160°C.[1]

Epoxide reactions were studied using FT-IR spectroscopy to determine the degree of crosslinking in Avatrel 8000P after each processing step. The IR spectra from 700 cm^{-1} to 950 cm^{-1} are shown in Fig. 12, and three peaks corresponding to asymmetric and symmetric epoxide ring stretches were observed at 913 cm^{-1}, 844 cm^{-1}, and 760 cm^{-1}. Between soft bake and post-exposure bake, minimal

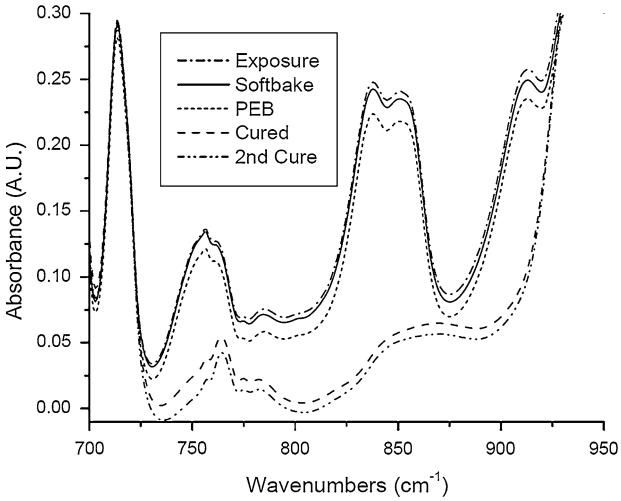

Fig. 12. Changes in FT-IR spectrum of Avatrel 8000P from 700 cm^{-1} to 950 cm^{-1} as a function of processing steps (soft bake: 100°C for 5 min; exposure: 500 mJ/cm^2; post-exposure bake: 100°C for 5 min; cure: 1 h at 225°C; second cure: 2 h at 250°C).

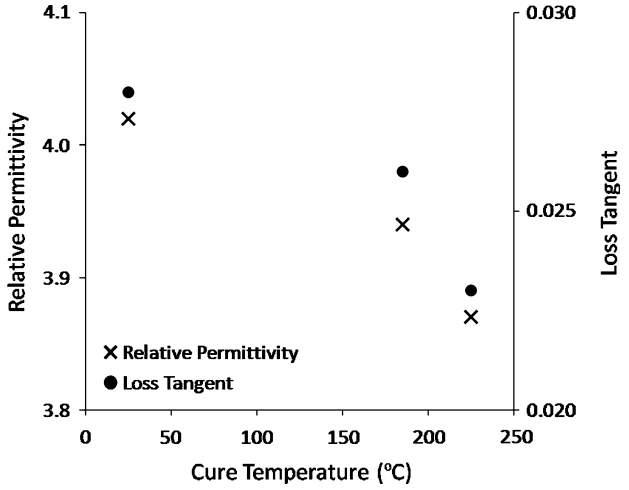

Fig. 13. Relative permittivity and loss tangent of Avatrel 8000P at cure temperatures of 25°C, 185°C, and 225°C.

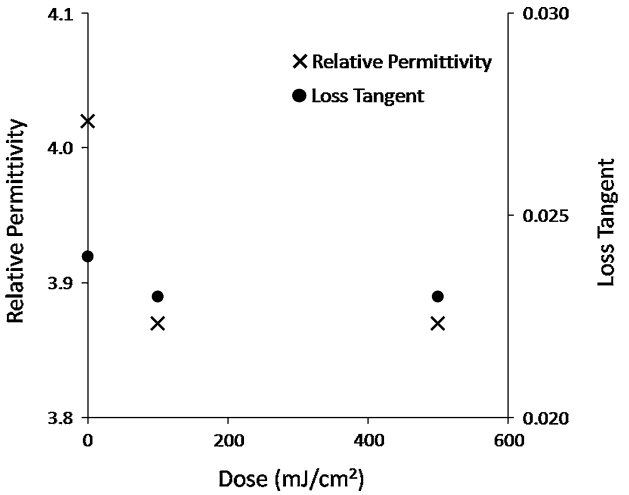

Fig. 14. Relative permittivity and loss tangent of Avatrel 8000P processed without an exposure dose, with an exposure dose of 200 mJ/cm^2, and with an exposure dose of 500 mJ/cm^2 and measured after post-exposure bake and cure at 225°C.

conversion of epoxy occurs, suggesting that little crosslinking has occurred. After curing at 225°C, the peak area at 844 cm^{-1} and 913 cm^{-1} disappeared, signifying that the epoxide rings have reacted and crosslinked with the polymer backbone. An extended cure of the same sample at 250°C for 2 h showed no significant change in the IR spectra, confirming that Avatrel 8000P curing reaction was complete.

The crosslinking reactions have a dramatic effect on the mechanical properties of Avatrel 8000P and also impact on the dielectric properties of the polymer. To evaluate the effect of crosslinking, the relative permittivity and loss tangent of cured Avatrel 8000P films were characterized for different processing conditions. For a fixed exposure dose of 500 mJ/cm^2, the loss tangent and dielectric constant decreased with increasing cure temperature, as shown in Fig. 13. The decrease in the dielectric constant at higher cure temperatures is likely due to a decrease in film polarizability (electron and dipole polarization) when the epoxy is completely cured. Since the C–O in the epoxy ring has a dipole moment of 0.7, which is higher than the dipole moment of the C–C (0.0) and C–H (0.4) bonds, complete reaction of the epoxy rings minimizes dipole polarization. Therefore, curing Avatrel 8000P at 225°C resulted in the lowest measured dielectric constant, $\varepsilon_r = 3.9$, which concurs with the high modulus of 2.9 GPa and a high extent of crosslinking.

To evaluate the impact of exposure dose, Avatrel 8000P samples were processed: (i) without an exposure dose, (ii) with an exposure dose of 200 mJ/cm^2 and (iii) with an exposure dose of 500 mJ/cm^2. All measurements were conducted after a post-exposure bake and cure at 225°C. Figure 14 shows that the unexposed Avatrel 8000P sample had a dielectric constant of 4.0 and loss tangent of 0.030, whereas the two samples that had UV exposure both had a dielectric constant of 3.9 and loss tangent of 0.023. In the unexposed Avatrel 8000P sample, a high concentration of unreacted epoxy groups resulted in an increase of overall dipole polarization and permittivity.[4]

The dielectric constant of fully cured Avatrel 2000P is 2.55[30] and the dielectric constant of SU-8 is 3.2,[14] which are both lower than the dielectric constant of Avatrel 8000P. The higher dielectric constant of Avatrel 8000P is first attributed to its polarizable side-groups: the fluorinated alcohol group and the carboxylic acid groups. Additionally, the multifunctional crosslinker additive also causes Avatrel 8000P to have a higher dielectric constant than Avatrel 2000P and SU-8.

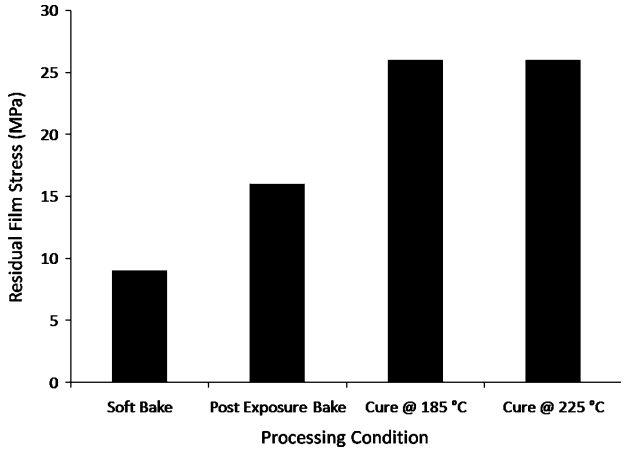

Fig. 15. Changes in internal film stress of Avatrel 8000P as a function of different processing conditions (soft-bake: 100°C for 5 min; post-exposure bake: 100°C for 5 min; cure 1: 185°C for 1 h; cure 2: 225°C for 1 h).

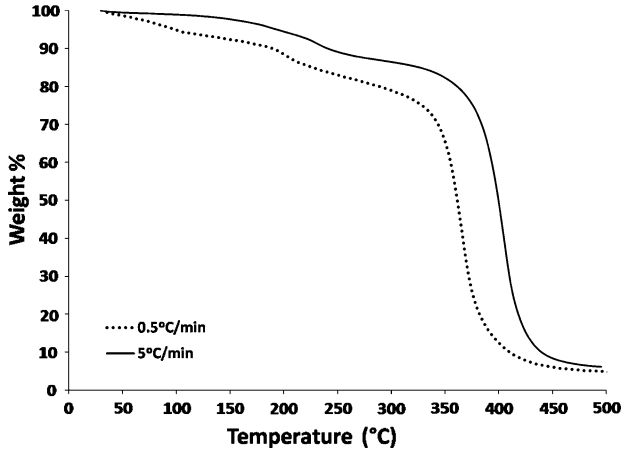

Fig. 16. Thermogravimetric analysis of Avatrel 8000P.

The residual stress of Avatrel 8000P films ranged from 9 MPa after soft bake to 26 MPa after curing, as shown in Fig. 15. After soft bake, residual stress in the film is primarily due to solvent removal. After post-exposure bake, the Avatrel 8000P film stress increases because UV exposure initiates catalyst mediated crosslinking. The high residual stress after cure is due to the high crosslink density of the polymer. Avatrel 2000P has a lower epoxy content and therefore lower residual stress values ranging from 2 MPa after soft-bake to 6 MPa after cure.[4] SU-8 which also has a high epoxy content has a residual stress of 18 MPa after post exposure bake which is comparable to Avatrel 8000P.[31]

In addition to mechanical integrity, a polymer film must also have a high level of thermal stability for successful implementation of polymer microstructures in MEMS and microelectronics applications. To evaluate the thermal stability of Avatrel 8000P, decomposition versus temperature of Avatrel 8000P was characterized through thermogravimetric analysis. Figure 16 shows thermogravimetric analysis of Avatrel 8000P at ramp rates of 0.5°C/min and 5°C/min. The apparent decomposition temperature shifts to lower values with slower ramp rates due to the reduced thermal lag between the sample and heat source.

CONCLUSION

Avatrel 8000P is a high-contrast, I-line-sensitive mixture that can be developed in traditional aqueous-base developers. The simple baking procedures make Avatrel 8000P easier to process than SU-8. Also, the ability to develop Avatrel 8000P in aqueous base can reduce chemical waste. As shown by SEM images, high-fidelity structures with aspect ratios of 7:1 and vertical side-walls can be fabricated in thick films. Avatrel 8000P and SU-8, which both have a high epoxy content, have comparable mechanical strength and residual stress. Avatrel 8000P's excellent photodefinition properties, high mechanical strength, and thermal stability make it suitable for MEMS and microelectronics packaging.

ACKNOWLEDGEMENTS

The authors gratefully acknowledge the support of Promerus LLC for providing materials for this research and many useful discussions. Thanks also to the Microelectronics Research Center and the Interconnect Focus Center for all of their help and support. The authors would also like to acknowledge the contributions of Shakira Charles for assistance with electrical measurements and Ryan Hart for help with FT-IR analysis.

REFERENCES

1. P. Chiniwalla, Y. Bai, E. Elce, R. Shick, W.C. McDougall, S.A. Bidstrup Allen, and P.A. Kohl, *J. Appl. Polym. Sci.* 89, 568 (2003). doi:10.1002/app.12234.
2. P. Chiniwalla, Y. Bai, E. Elce, R. Shick, S.A. Bidstrup Allen, and P.A. Kohl, *J. Appl. Polym. Sci.* 91, 1020 (2004). doi:10.1002/app.13045.
3. Y. Bai, P. Chiniwalla, E. Elce, S.A. Bidstrup Allen, and P.A. Kohl, *J. Appl. Polym. Sci.* 91, 3031 (2004). doi:10.1002/app.13530.
4. Y. Bai, P. Chiniwalla, E. Elce, R. Shick, J. Sperk, S.A. Bidstrup Allen, and P.A. Kohl, *J. Appl. Polym. Sci.* 91, 3023 (2004).
5. R. Feng and R.J. Farris, *J. Micromech. Microeng.* 13, 80 (2003).
6. J.M. Shaw, J.D. Gelome, N. Labianca, W.E. Conley, and S.J. Holmes, *IBM J. Res. Dev.* 41, 81 (1997).
7. J.D. Gelorme, R.J. Cox, and S.A.R. Gutierrez, International Business Machines Corporation (IBM), U.S. patent no. 4,882,245 (1989).
8. K.Y. Lee, N. LaBianca, and S.A. Rishton, *J. Vac. Sci. Technol. B* 13, 3012 (1995).
9. N. Labianca et al., *Elecrochem. Soc. Proc.* 95-18, 386 (1993).
10. A. Bertsch, H. Lorenz, and P. Renand, *IEEE Micro. Electro. Mech. Syst.* (1998), p. 18.
11. M. Despont, H. Lorenz, N. Fahrni, J. Brugger, P. Renaud, and P. Vettiger, *10th IEEE Micro. Electro. Mech. Syst.* (1997), p. 518.
12. H. Lorenz, M. Laudon, and P. Renaud, *Microelectron. Eng.* 41–42, 371 (1988).
13. H. Lorenz, M. Despont, N. Fahrni, N. Labianca, P. Renaud, and P. Vettiger, *Macromech. Microeng.* 7, 121 (1997).

14. MicroChem Website, http://www.microchem.com/products/pdf/SU-82000DataSheet2000_5thru2015Ver4.pdf (2008).
15. W.C. Oliver and G.M. Pharr, *J. Mater. Res.* 7, 1564 (1992).
16. American Society for Testing and Materials, *Standard Test Methods for AC Loss Characteristics and Permittivity (Dielectric Constant) of Solid Electrical Insulating Materials* (Philadelphia, PA, 1992).
17. C.A. Klein, *J. Appl. Phys.* 88, 5487 (2000).
18. J.L. Loubet, J.M. Georges, O. Marchesini, and G. Meille, *J. Tribol.-T. ASME* 106, 43 (1984).
19. S. Jiang, X. Li, S. Guo, Y. Hu, J. Yang, and Q. Jiang, *Smart Mater. Struc.* 14, 769 (2005).
20. G.A. Shaw, J.S. Trethewey, A.D. Johnson, W.J. Drugan, and W.C. Crone, *Adv. Mater.* 17, 1123 (2005).
21. Z.Y. Yuan, D. Zu, Z.C. Ye, and B.C. Cai, *J. Mater. Sci. Technol.* 21, 319 (2005).
22. M.R. VanLandingham, J.S. Villarrubia, W.F. Guthrie, and G.F. Meyers, *Macromol. Symp.* 167, 15 (2001).
23. B.J. Briscoe, L. Fiori, and E. Pelillo, *J. Phys. D Appl. Phys.* 31, 2395 (1998).
24. L. Shen, I.Y. Phang, T.X. Liu, and K.Y. Zeng, *Polymer* 45, 8221 (2004).
25. E. Wornyo, K. Gall, F. Yang, and W. King, *Polymer* 48, 3213 (2007).
26. C. Klapperich, K. Komvopoulos, and L. Pruitt, *J. Tribol-T. ASME* 123, 624 (2001).
27. Micro Chemwebsite, http://www.microchem.com/products/su_eight_faq.htm (2009).
28. B. Eyre, J. Blosiu, and D. Wiberg, *11th IEEE Micro. Elec. Mech. Syst.*, Chicago, USA (1995), p. 218.
29. T.C. Osborn, H. Lighsety, and P.A. Kohl, *Microelectron. Eng.* (2009). doi:10.1016/j.mee.2008.11.080.
30. K. Patel, P.A. Kohl, and S.A. Bidstrup Allen, *J. Appl. Polym. Sci.* 80, 2328 (2001).
31. J. Hammacher, A. Fuelle, J. Flaemig, J. Saupe, B. Loechel, and J. Grimm, *Microsyst. Technol.* 14, 1515 (2008).